Self-Assembly of Monolayers of Semiconductor Nanocrystallites

Rosalba Rizza and Donald Fitzmaurice*

Department of Chemistry, University College Dublin, Dublin 4, Ireland

Sean Hearne and Greg Hughes

School of Physical Sciences, Dublin City University, Dublin 9, Ireland

Giuseppe Spoto and Enrico Ciliberto

Dipartimento di Scienze Chimiche, Universita' di Catania, Viale Andrea Doria 6, 95125 Catania, Italy

Harald Kerp and Ruud Schropp

Department of Interface Physics, Utrecht University, P.O. Box 80000, 3508 TA Utrecht, The Netherlands

Received May 9, 1997. Revised Manuscript Received August 13, 1997[⊗]

Described is the self-assembly of a monolayer of TiO_2 nanocrystallites on a gold substrate by two related methods. In the first of these methods, a crystalline monolayer of the functionalized thiol $HS-(CH_2)_{10}-COOH$ is self-assembled at an annealed gold substrate by adsorption from ethanolic solution. The modified gold substrate is then immersed in an ethanolic TiO_2 colloid. TiO_2 nanocrystallites are adsorbed at the terminal −COOH group of the molecules constituting the monolayer. In the second of these methods, an ethanolic colloid of TiO_2 nanocrystallites is prepared in the presence of the functionalized thiol $HS-(CH_2)_{10}-COOH$. The modified nanocrystallites are adsorbed at the surface of an annealed gold substrate. For each method, there is some evidence for short-range ordering of the nanocrystallites constituting the close-packed monolayer adsorbed at the gold substrate. Some potential applications of these methods are considered.

Introduction

The recent past has seen increased interest in the preparation of and characterization of nanoporous−nanocrystalline semiconductor electrodes.[1] This interest is, in large part, a result of the development of highly efficient regenerative photoelectrochemical cells based on dye-sensitized nanoporous−nanocrystalline semiconductor electrodes.[2] Further interest has been generated by the development of electrochromic and photochromic windows, lithium insertion batteries, and hybrid solar cell−electrochromic window devices based on nanoporous−nanocrystalline semiconductor electrodes.[3] In short, a range of technologically important applications for such electrodes are emerging, while others are foreseen.

Concerning the characterization of nanoporous−nanocrystalline semiconductor electrodes, hereafter referred to as nanostructured electrodes, two aspects of these materials have received particular attention.[4] First, the extent of charge carrier accumulation or depletion, if any, that exists at a given applied potential; second, the mechanism of charge-carrier transport leading to accumulation or depletion under the same conditions. The widespread interest in these questions arises, first, from the apparent differences between nanostructured and conventional single-crystal electrodes in these respects, and second, from the need to understand these processes in order to optimize the increasing number of commercially important devices based on nanostructured electrodes. However, despite a large number of studies utilizing a wide range of techniques, it is clear that an agreed view on these matters has yet to emerge.

One of the principal difficulties encountered in attempting to address the above issues has been the

* To whom correspondence should be addressed.

[⊗] Abstract published in *Advance ACS Abstracts,* October 1, 1997.

(1) Hagfeldt, A.; Grätzel, M. *Chem. Rev. (Washington, D.C.)* **1995**, *95*, 49.

(2) O'Regan, B.; Grätzel, M. *Nature* **1991**, *353*, 737.

(3) (a) Marguerettaz, X.; O'Neill, R.; Fitzmaurice, D. *J. Am. Chem. Soc.* **1994**, *116*, 2629. (b) Hagfeldt, A.; Vlachopoulos, N.; Grätzel, M. *J. Electrochem. Soc.* **1994**, *141*, L82. (c) Bonhote, P.; Moser, J.; Vlachopoulos, N.; Walder, L.; Zakeeruddin, S.; Humphry-Baker, R.; Pechy, P.; Grätzel, M. *Chem. Commun.* **1996**, 1166. (d) Bechinger, C.; Ferrere, S.; Zaban, A,; Sprague, J.; Gregg, B. *Nature* **1996**, *383*, 608.

(4) (a) O'Regan, B.; Grätzel, M.; Fitzmaurice, D. *J. Phys. Chem.* **1991**, *95*, 10525. (b) Redmond, G.; Grätzel, M.; Fitzmaurice, D. *J. Phys. Chem.* **1993**, *97*, 6951. (c) Hotchandani, S.; Kamat, P. *J. Phys. Chem.* **1992**, *96*, 6834. (d) Liu, D.; Kamat, P. *J. Phys. Chem.* **1993**, *97*, 10769. (e) Hotchandani, S.; Kamat, P. *J. Electrochem. Soc.* **1992**, *139*, 1630. (f) Hodes, G.; Albu-Yaron, A. *Proc. Electrochem. Soc.* **1988**, *88*, 298. (f) Hodes, G.; Howell, I.; Peter, L. *J. Electrochem. Soc.* **1992**, *139*, 3136. (g) Lyons, A.; Hupp, J. *J. Phys. Chem.* **1995**, *99*, 15718. (h) Schwarzburg, K.; Willig, F. *Appl. Phys. Lett.* **1991**, *58*, 2520. (i) Willig, F; Kietzmann, R.; Schwarzburg, K. *Photochemical and Photoelectrochemical Conversion and Storage of Solar Energy*; Tian, Z., Cao, Y., Eds.; International Academic Publishers: Beijing, 1993; p 129. (j) Lindquist, S.-E.; Finnstrom, B.; Tegner, L. *J. Electrochem. Soc.* **1983**, *130*, 351. (k) Hagfeldt, A.; Bjorksten, U.; Lindquist, S.-E. *Sol. Energy Mater. Sol. Cell.* **1992**, *27*, 293. (l) Sodergren, S.; Hagfeldt, A.; Olsson, J.; Lindquist, S.-E. *J. Phys. Chem.* **1994**, *98*, 5552.

S0897-4756(97)00349-9 CCC: $14.00

Scheme 1

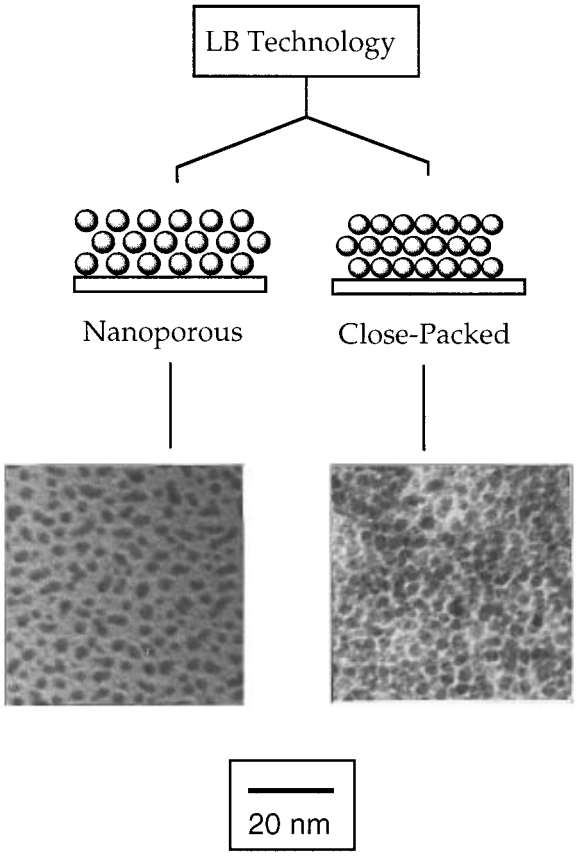

absence of well-defined nanostructured electrodes. That is, electrodes constituted from nanocrystallites possessing well-defined properties and organized in a well-defined manner. The availability of such electrodes would allow the following difficulties to be addressed: First, the results of the wide range of experimental techniques applied to the study of nanostructured electrodes could be compared. Second, the resulting models for charge-carrier transport leading to accumulation or depletion could be tested by systematically varying the properties and organization of the nanocrystallites constituting the nanostructured electrode. Finally, these findings could be expected to form the basis of a systematic optimization of the nanostructured electrodes on which devices such as those referred to above are based.[3]

Toward this end we have recently described the preparation of nanostructured TiO_2 electrodes possessing well-defined morphologies from nanocrystallites whose properties are also well defined.[5] Briefly, Langmuir−Blodgett techniques were used to deposit between one and four monolayers of TiO_2 nanocrystallites (22 ± 2 Å) on conducting glass. As the average spacing between the nanocrystallites constituting a deposited monolayer could be controlled, the porosity of the resulting nanocrystalline film was determined. Subsequent firing, fusing the constituent crystallites of the deposited monolayers, ensured an ohmic contact with the conducting substrate. Characterization by electron microscopy revealed the above films to be nanoporous or close-packed arrays of anatase nanocrystallites; see Scheme 1. Measurement of potential-dependent optical

(5) Doherty, S.; Fitzmaurice, D. *J. Phys. Chem.* **1996**, *100*, 10732.

Scheme 2

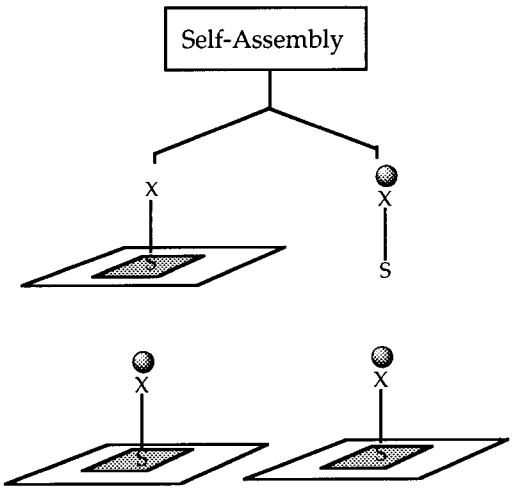

absorption spectra suggests that the degree of charge-carrier accumulation possible at a given applied potential is dependent on the morphology of the nanostructured electrode. These studies are currently being extended.[6]

The above findings represent an advance in the preparation of nanostructured TiO_2 electrodes possessing well-defined morphologies and may prove useful in understanding the factors determining the extent, if any, of charge-carrier accumulation or depletion at a given applied potential.[6] In relation to the study of charge-carrier transport however, the nanostructured electrodes in Scheme 1 continue to represent a complex substrate. Consequently, nanostructured electrodes constituted from equally well-defined nanocrystallites, but possessing still simpler morphologies, are required. The use of appropriately modified substrates to template the self-assembly of patterned monolayers of TiO_2 nanocrystallites is being considered in this context.

It is noted that a number of reports have described the self-assembly of monolayers of metal or semiconductor nanocrystallites at a modified substrate.[7] Two principal approaches have been adopted. In the first of these, a two-step method, a bifunctional molecule is adsorbed at an unmodified substrate to form an organized monolayer at which unmodified nanocrystallites are subsequently adsorbed; see Scheme 2. In the second, a one-step method, nanocrystallites modified by adsorption of a bifunctional molecule are adsorbed at the surface of an unmodified substrate; see Scheme 2. Closely related studies, in which a thin film of Ti has been deposited on an organic monolayer or a thin film of TiO_2 has been self-assembled at an organic monolayer, are also noted.[8]

This paper describes the self-assembly of a monolayer of TiO_2 nanocrystallites on a Au substrate by each of

(6) Boschloo, G.; Fitzmaurice, D., manuscript in preparation.

(7) (a) Colvin, V.; Goldstein, A.; Alivisatos, P. *J. Am. Chem. Soc.* **1992**, *114*, 5221. (b) Kotov, N.; Dékány, I.; Fendler, J. *J. Phys. Chem.* **1995**, *99*, 13065. (c) Doron, A.; Katz, E.; Willner *Langmuir* **1995**, *11*, 1313. (d) Freeman, R.; Grabar, K.; Allison, K.; Bright, R.; Davis, J.; Guthrie, A.; Hommer, R.; Jackson. M.; Smith, P.; Walter, D.; Natan, M. *Science* **1995**, *267*, 1629.

(8) (a) Konstadinidis, K.; Zhang, P.; Opila, R.; Allara, D. *Surf. Sci.* **1995**, *338*, 300. (b) Shin, H.; Collins, R.; De Guire, M.; Heurer, A.; Sukenik *J. Mater. Res.* **1995**, *10*, 692. (c) Shin, H.; Collins, R.; De Guire, M.; Heurer, A.; Sukenik *J. Mater. Res.* **1995**, *10*, 699.

Scheme 3[a]

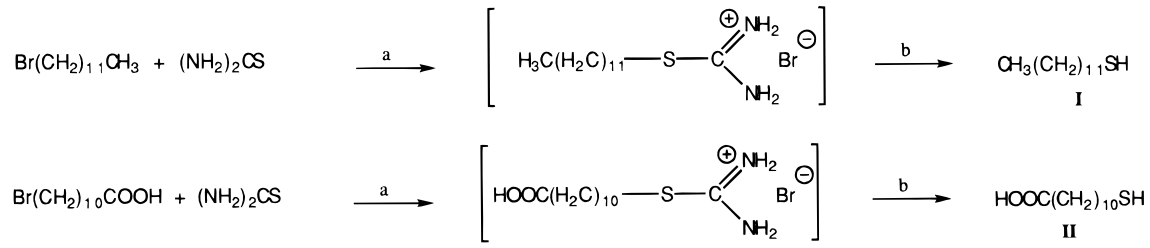

[a] EtOH reflux. [b]Aqueous NaOH reflux.

the methods outlined above and shown in Scheme 2. Specifically, a crystalline monolayer of the functionalized thiol $HS-(CH_2)_{10}-COOH$ is self-assembled at an annealed Au substrate by adsorption from ethanolic solution. The modified Au substrate is then immersed in an ethanolic TiO_2 colloid. TiO_2 nanocrystallites are adsorbed at the terminal $-COOH$ group of the molecules constituting the monolayer. Alternately, an ethanolic colloid of TiO_2 nanocrystallites is prepared in the presence of the functionalized thiol $HS-(CH_2)_{10}-COOH$. The modified nanocrystallites are then adsorbed at the surface of an annealed Au substrate. For each method, there is some evidence for short-range ordering of the nanocrystallites constituting the close-packed monolayer adsorbed at the gold substrate. Some potential applications of these methods are considered.

Experimental Section

Synthesis and Characterization of Functionalized Thiols. Compounds **I** and **II** were synthesized as shown in Scheme 3 and characterized by ^1H NMR and elemental analysis.

Calculated for **I** ($C_{12}H_{26}S$): C, 71.21; H, 12.95; S, 15.84. Found: C, 71.27; H, 13.22; S, 15.95. ^1H NMR ($CDCl_3$) δ 0.88 (t, 3H, $J = 6.7$), 1.26−1.36 (unresolved m, 18H), 1.61 (q, 2H, $J = 7.3$ Hz), 2.52 (q, 2H, $J = 7.5$ Hz).

Calculated for **II** ($C_{11}H_{22}O_2S$): C, 60.56; H, 10.08; S, 14.05. Found: C, 61.17; H, 10.39; S, 14.10. ^1H NMR ($CDCl_3$) δ 1.23−1.36 (unresolved m, 12H), 1.60 (unresolved m, 4H), 2.34 (t, 2H, $J = 7.5$ Hz), 2.52 (q, 2H, $J = 7.5$ Hz).

Preparation and Characterization of Semiconductor Nanocrystallites. Nanocrystallites used in the present study were prepared as follows: 1.0 mL of titanium tetraisopropoxide was added to 9.0 mL of propanol. The above stock solution (0.6 mL) was added with vigorous stirring and in the dark to 50 mL of absolute ethanol during 1 h. The resulting concentration of TiO_2, assuming complete conversion, was 4.1×10^{-3} mol dm^{-3} or 0.326 g/L. Alternately, 0.6 mL of the above stock solution was added with vigorous stirring and in the dark to 50 mL of absolute ethanol during 1 h containing 4.1×10^{-4} mol dm^{-3} or 0.087 g/L of **II**.

Preparation and Characterization of Gold Substrate. A polished/etched p-type Si (100) wafer was cut into 30 mm × 20 mm slides. These slides were cleaned using the procedure reported by Lee et al. and placed in a vacuum deposition chamber.[9] A layer of Au was deposited by thermal evaporation at a rate of 1 Å/s to a final thickness of 600 Å and annealed in air at 250 °C for 3 h.

Preparation and Characterization of Adsorbed Monolayers of Functionalized Thiols and Semiconductor Nanocrystallites. A freshly annealed Au substrate was placed in a 1.0×10^{-2} mol dm^{-3} ethanolic solution of **I** or **II** for 24 h, washed thoroughly with ethanol, and dried in a stream of dry nitrogen. The modified Au substrate was immersed in an ethanolic dispersion of TiO_2 nanocrystallites for 4 h, washed thoroughly with ethanol, and dried in a stream of dry nitrogen.

Characterization of Organized Organic Monolayers and Adsorbed Semiconductor Nanocrystallites. The thickness of a deposited organic layer was determined by ellipsometry.[10] Specifically, a S. A. Jobin Yvon UVISEL variable-angle spectroscopic phase-modulated ellipsometer was used at an angle of incidence of 75° and over the wavelength range 275−775 nm. The complex refractive indexes for the substrates were calculated using a two-phase parallel-layer model from classical electromagnetic theory. After adsorption of an organized monolayer of **I** or **II**, the sample was again analyzed and the film thickness determined from a three-phase model. A value of 1.46 for the refractive index was used for the monolayer since the imaginary part of the complex refractive index is zero at over the spectral range studied, i.e., both **I** and **II** are transparent at these wavelengths. The complex refractive indexes measured above were used for the substrate.

Infrared reflection−absorption spectra were recorded using a Fourier transform infrared (FTIR) spectrometer (Mattson Infinity) equipped with a liquid nitrogen cooled MCT detector. Specifically, polarized reflection spectra were recorded using a variable-angle reflection accessory (Graseby-Specac P/N 19650) mounted in the sample compartment of the FTIR spectrometer. The final spectrum was obtained by coaddition of 10^4 scans recorded under a nitrogen purge at 2 cm^{-1} resolution using p-polarized light (wire-grid polarizer) with an incident angle of 85°. A background was recorded, under the same conditions, for a given substrate prior to modification.

Also recorded were transmission FTIR spectra of **I** and **II** in the crystalline state. The final spectrum was obtained by coaddition of 10^2 scans recorded under a nitrogen purge at 1 cm^{-1} resolution. In the case of **I**, a liquid at room temperature, the crystalline state spectrum was recorded in a variable-temperature infrared cell at −10 °C. It should be noted that this spectrum was recorded for a sample that had been repeatedly annealed and for which no further increase in the ordering in the crystalline solid could be detected spectroscopically. The concentration of **I** was assumed to be the molar concentration of the pure solid at −10 °C. The optical path length was determined interferometrically. In the case of **II**, a solid a room temperature, the crystalline-state spectrum was measured for a known concentration of the crystalline compound in a KBr pellet (0.05 mg of **II** in 100.00 mg of KBr). The optical path length was determined by measurement of the thickness of the pellet.

Survey X-ray photoelectron spectra (XPS) were recorded at a takeoff angle of 15° using a system that consisted of a CLAM 100 electron energy analyzer and an X-ray source, both from VG Scientific. The Kα X-ray line (1486.6 eV) of aluminum at a spectrometer pass energy of 50 eV was used as the source. The survey spectra reported were recorded with a step resolution of either 1.0 or 0.2 eV.

High-resolution XPS spectra were recorded at takeoff angles of 45°, 15°, 5°, 3°, and 1° using a Perkin-Elmer PHI ESCA/SAM 5600 spectrometer equipped with a spherical capacitor energy analyzer. The Kα X-ray line (1486.6 eV) of aluminum

(9) Lee, H.; Kepley, L.; Hong, H.; Akhter, S.; Mallouk, T. *J. Phys. Chem.* **1988**, *92*, 2597.

(10) The authors wish to thank the staff of the National Microelectronics Research Centre, and in particular Dr. Patrick Kelly, for their assistance in undertaking the reported ellipsometric studies.

at a spectrometer pass energy of 11.75 eV and step resolution of 0.1 eV was used as the source. The above configuration gave an instrument resolution of 1.0 eV. The measured spectra were referenced to the Au $4f_{7/2}$ peak at 84.0 eV. In fitting the high-resolution spectra measured as described above, a 80% Gaussian/20% Lorentzian peak profile was used.

Rutherford backscattering spectra (RBS) were recorded using He^+ (2 MeV) for samples whose surface is at 50° to the incident beam.

Scanning tunneling micrographs (STMs) were recorded in air at room temperature using a Nanoscope II (Digital Instruments) and Pt−Ir tips (Digital Instruments). The Nanoscope II was operated in constant height mode for all samples at scan rates in the range 2.0−3.5 Hz. A positive sample bias voltage of +100 mV was always used in conjunction with an initial set point tunnel current of 1 nA to establish a fixed height for the sample above the surface.

Transmission electron micrographs (TEMs) were obtained using a JEOL 2000FX TEMSCAN. Electron diffraction (ED) patterns were obtained under the same conditions. Samples to be studied were prepared on a 200 Å thick Au (111) layer deposited on a Si (100) wafer and annealed, both as described above. Modified Au films were subsequently removed from the Si substrate by treatment with a dilute aqueous solution of NaOH and KCN in a trough and floated on to a 400-mesh copper grid.

X-ray diffraction (XRD) patterns were obtained using a Phillips PW 1730 Series system.

Simulation of the Measured Reflection−Absorption Spectra. The isotropic optical constants, n and k in eq 1, were obtained for **I** and **II** in the crystalline state from the transmission infrared spectra measured as described above.

$$\hat{n} = n + ik \tag{1}$$

The method has been described by Allara et al. and is summarized below.[11] The imaginary part of the complex refractive index $k(\bar{\nu})$ was approximated using eq 2, the Beer−Lambert law:

$$T/T_0 = \exp(-4\pi k' d_z \bar{\nu}) \tag{2}$$

T and T_0 are the intensities of the light transmitted by a KBr disk containing either **I** or **II** and a KBr disk containing neither **I** or **II** respectively, d_z is the pellet thickness, and $\bar{\nu}$ the wavenumber.

$k'(\bar{\nu})$ is given by eq 3 where C and C_0 are the concentration of **I** or **II** in the spectroscopic sample and in the crystalline state, respectively.

$$k'(\bar{\nu}) = k(\bar{\nu})C/C_0 \tag{3}$$

The real part $n(\bar{\nu})$ was calculated using the Kramer−Kronig transform given by eq 4.[12] This initial set of values for $n(\bar{\nu})$

$$n(\bar{\nu}_i) = n_\infty + \frac{1}{\pi}\int_{\bar{\nu}_1}^{\bar{\nu}_2} \frac{k(\bar{\nu})\bar{\nu}\, d\bar{\nu}}{(\bar{\nu}^2 - \nu_i^2)} \tag{4}$$

and $k(\bar{\nu})$ were used in a Fresnel model for multiple layers to evaluate the transmittance for **I** and **II**.[13] This yielded sets of values for $k(\bar{\nu})$ that were almost identical with the initial values. The self-constancy of these data sets was taken as confirming the validity of the Beer−Lambert approximation.

To construct the required optical tensor, the $k(\bar{\nu})$ spectrum was resolved into 10 separate contributions from isolated excited modes with a prior knowledge of the individual modes contributing to a given peak. The characteristic frequencies and band shapes reported in the literature were used initially.[14] Each mode was arbitrarily assumed to be a mixture of 60/40 Gaussian/Lorentzian band shape. A least-squares routine was used to resolve the different modes with the free parameters being the intensity of each mode and the full width at half-maximum (fwhm).

To take into account the specific orientation of the adsorbate on the surface, the scalar function $\hat{n}(\bar{\nu})$ was transformed into a tensor $\tilde{n}(\bar{\nu})$ as described by Parikh et al.[15] Briefly, the resolved k values are scaled by a factor that represents the cosine direction of a given oscillator in the experimental coordinate system. This was achieved using a rotational matrix representing the tilt (α), twist (β), and azimuth (ψ) angle in the experimental coordinate system.[16]

The simulation of the reflection infrared spectrum for a given orientation of a monolayer of **I** or **II** on a Au substrate is based on the assumption that the above monolayer is a collection of uniformly oriented molecules forming a crystalline thin film. Specifically, a FORTRAN algorithm is used to calculate the propagation of an electromagnetic wave through an anisotropic three-layer medium (air/organic monolayer/gold). The above FORTRAN code, based on that developed by Parikh et al. and based on the 4 × 4 matrix formalism developed by Yeh's et al.,[15,17] has been adapted for our own use.[18] The thickness of each layer (determined from ellipsometric studies), the optical tensor for an assumed orientation of the organic monolayer, the tensors for the Au and air layers were used as input parameters for the calculation and adjusted until the best fit between the recorded spectra and the simulated one was obtained.

Results and Discussion

Characterization of TiO_2 Nanocrystallites. The bandgap energy E_g, assigned to the lowest energy indirect transition of nanocrystallites prepared in the absence of **II**, is 3.1 ± 0.1 eV. This value is determined from a plot of $(\alpha h\nu)^{1/2}$ versus $h\nu$ as shown in Figure 1a.[19] The absorption coefficient α is given by eq 5, where B_i

$$\alpha = B_i(h\nu - E_g)^2/h\nu \tag{5}$$

is the absorption constant for an indirect transition and E_g is the corresponding bandgap energy. α is calculated according to eq 6, where A is the measured absorbance,

$$\alpha = 2.303 \times 10^3 A\rho/lc \tag{6}$$

ρ is the density of the semiconductor (3.89 g cm^{-3} for anatase), l is the optical path length (1.0 cm), and c is the concentration of TiO_2 (0.326 g dm^{-3}).[20]

According to a recent report by Serpone et al. this would suggest a particle diameter greater than 21 ± 2 Å.[21] This suggestion is supported by the transmission electron micrograph shown in Figure 1b, from which the average particle diameter is determined to be 22 ± 4 Å. On this basis, the particle concentration was calcu-

(11) Allara, D.; Nuzzo, R. *Langmuir* **1985**, *1*, 52−65.
(12) Arfken, G. *Mathematical Methods for Physicists*; Academic Press: San Diego, 1985; pp 421−424.
(13) Heavens O. *Optical Properties of Thin Films*; Dover Publications: New York, 1991; pp 74−77.
(14) MacPhail R.; Strauss, H.; Snyder, R.; Elliger C. *J. Phys. Chem.* **1984**, *88*, 334.
(15) Parikh, A.; Allara D. *J. Chem Phys.* **1992**, *96*, 927.
(16) Wilson, E.; Decius J.; Cross, P. *Molecular Vibrations*; McGraw-Hill: New York, 1955; pp 285−286.
(17) Yeh, P. *Surf. Sci.* **1980**, *96*, 41.
(18) The authors wish to thank Drs. Allara, Heitpas, and Parikh for their assistance in modifying their algorithm and the corresponding program for use in the studies reported here. The above algorithm may be downloaded by logging onto london@mrl.psu.edu with the user id "ir" and the password "public".
(19) Pankov, J. *Optical Processes in Semiconductors*; Dover: New York, 1971; Chapter 3.
(20) Delgass, W.; Haller, G.; Kellerman, R.; Lunsford, J. *Spectroscopy in Heterogeneous Catalysis*; Academic Press: New York, 1979; p 128.
(21) Serpone, N.; Lawless, D.; Khairutdinov, R. *J. Phys. Chem.* **1995**, *99*, 16646.

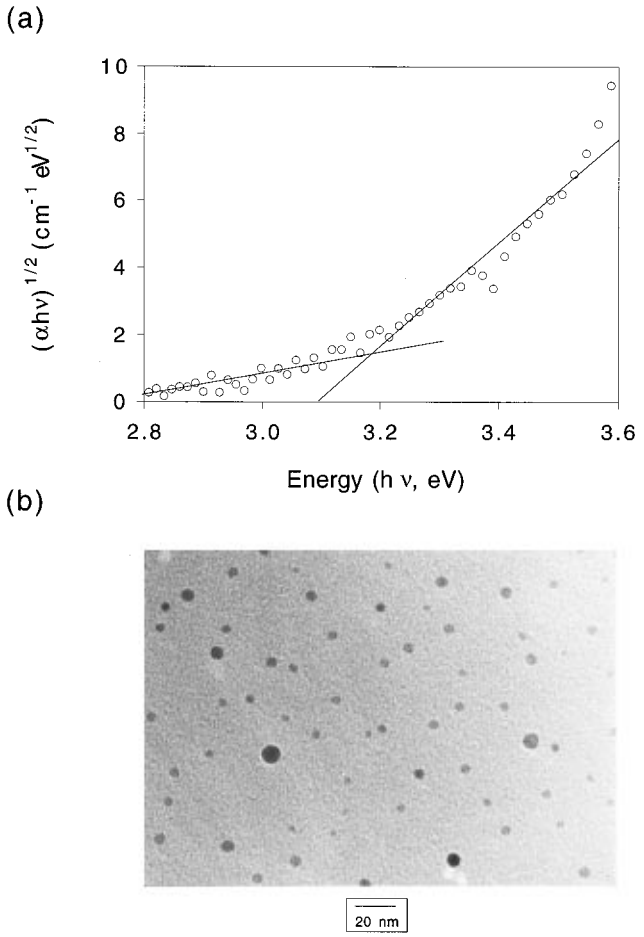

Figure 1. (a) Determination of the energy of lowest energy indirect transition of TiO_2 (anatase) nanocrystallites constituting a typical ethanolic colloid prepared in the absence of HS−$(CH_2)_{10}$−COOH. (b) A transmission electron micrograph of the TiO_2 nanocrystallites (average diameter 46 ± 4 Å) constituting the colloid in (a).

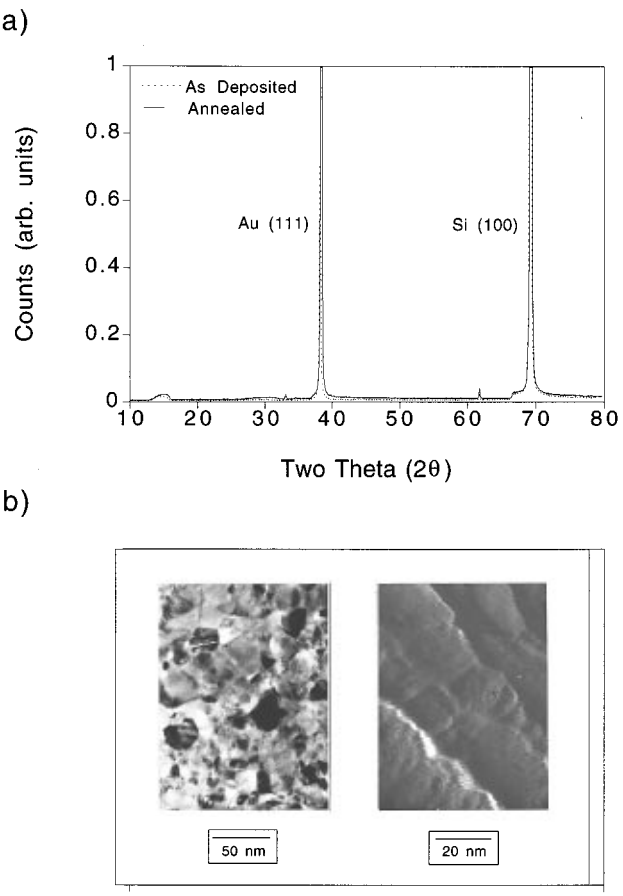

Figure 2. (a) X-ray diffraction spectrograph of a Si (100) wafer coated with a 600 Å thick Au (111) film prior to and following annealing at 250 °C for 3 h. (b) Transmission electron (left) and scanning tunneling (right) micrographs of the annealed sample in (a).

lated to be 3×10^{-5} mol dm^{-3}. The corresponding electron diffraction pattern confirms the particles shown in Figure 1b are nanocrystallites of TiO_2 (anatase). The following d_{hkl} values were obtained in angstroms: 3.5 (3.52); 2.4 (2.43); 2.4 (2.37); 2.3 (2.32); 1.9 (1.89); 1.7 (1.70); 1.7 (1.67). The expected values are those in brackets.[22]

Similar results were obtained for nanocrystallites prepared in the presence of **II**. Specifically, E_g and the average diameter were determined to be 3.1 ± 0.1 eV and 20 ± 4 Å, respectively, and these nanocrystallites were shown to be anatase. Using the above average particle diameter, the particle concentration was calculated to be 2×10^{-5} mol dm^{-3}. This implies there are 20 molecules of **II** per nanocrystallite and that the surface area available for adsorption of each is an ample 64 Å^2/molecule. We note the smaller size of the above nanocrystallites is likely due to their being capped.

Characterization of Gold Substrate. X-ray diffraction confirms that the Si substrate and deposited Au layer have (100) and (111) orientations, respectively, and that the crystallinity of the deposited Au layer increases upon annealing; see Figure 2a.[22] Characterization by transmission electron microscopy and scanning tunneling microscopy shows the annealed films consist of submicron domains and that these domains possess atomically flat terraces extending over some tens of nm; see Figure 2b. These findings are largely consistent with those recently reported by Golan et al.[23]

Characterization of Self-Assembled Monolayers of Functionalized Thiols. The monolayers of **I** and **II** self-assembled at the annealed Au surface, whose preparation and characterization are described above, were characterized by ellipsometry and reflection−absorption infrared spectroscopy.

The average thickness of the deposited layers, as determined from ellipsometric studies, is 20 ± 2 and 23 ± 2 Å for **I** and **II**, respectively. It is noted these values are in good agreement with those predicted for monolayers of **I** and **II** normal to the Au substrate of 19.9 and 19.5 Å, respectively.[24] These values also agree well with those previously reported for **I** (21 ± 3 Å) and closely related molecules.[25] Together these results suggest a monolayer of **I** and **II** is present in each case.

To more completely characterize the monolayers of **I** and **II** formed on the Au substrate the surface reflec-

(22) Holzer, J.; McCarthy, G. North Dakota State University, JCPDS Grant-in-Aid Report. 1990.

(23) Golan, Y.; Margulis, L.; Matlis, S.; Rubinstein, I. *J. Electrochem. Soc.* **1995**, *142*, 1629.

(24) Energy minimised structures of the thiols **I** and **II** were obtained using SPARTAN (AM-1). The distances given were determined from the above.

(25) Porter, M.; Bright, T.; Allara, D.; Chidsey, C. *J. Am. Chem. Soc.* **1987**, *109*, 3559.

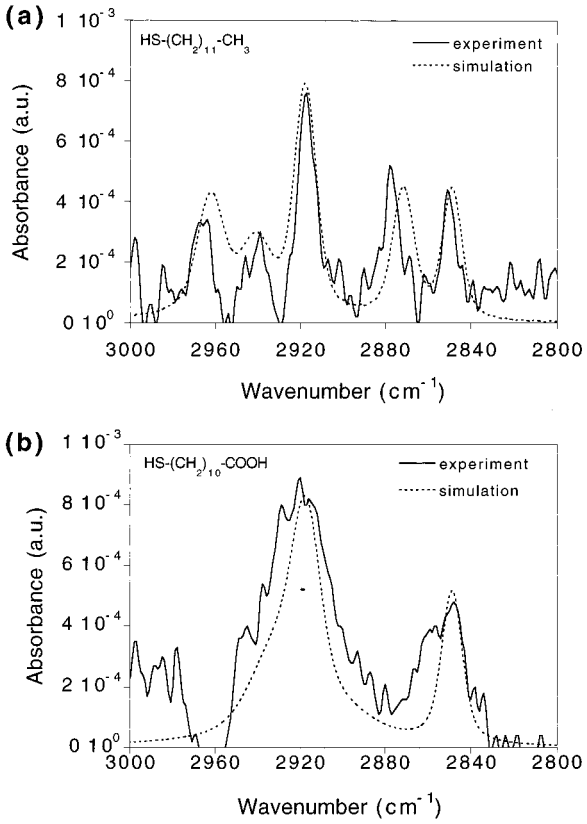

Figure 3. (a) Surface reflection−absorption infrared spectrum, measured using p-polarized light at an incident angle of 85°, of a crystalline monolayer of $HS-(CH_2)_{11}-CH_3$ adsorbed at an annealed Au substrate similar to that in Figure 2. Also shown is the simulated spectrum. (b) As in (a) for a crystalline monolayer of $HS-(CH_2)_{10}-COOH$ adsorbed at an annealed Au substrate similar to that in Figure 2.

tion−absorption infrared spectra shown in Figure 3 were recorded using p-polarized light. The principal feature in the 3000−2800 cm^{-1} region of the measured spectra is the asymmetric $-CH_2-$ stretch at 2918 ± 1 cm^{-1} (0.0006 ± 1 au) and 2920 ± 1 cm^{-1} (0.0005 ± 1 au) for **I** and **II**, respectively.[16,25]

Porter et al. have previously reported that for a close-packed crystalline monolayer of **I** adsorbed at a Au surface, the measured absorbance at 2919 cm^{-1} under the same conditions is 0.0006 au.[25] These values, being in excellent agreement with those determined from Figure 3a and summarized in Table 1, confirm that a crystalline-like monolayer of **I** is adsorbed at the Au substrate. Since **II** contains one less $-CH_2-$ unit than **I**, it would be expected, as observed in Figure 3b, that the measured absorbance is proportionately smaller than that observed for a monolayer of **I**. Further, the frequency of the asymmetric stretch also lies, as expected, between that observed for **I** (2919 cm^{-1}) and the corresponding *n*-alkylthiol containing nine $-CH_2-$ units (2920 cm^{-1}). In short, these findings also confirm that a crystalline monolayer of **II** is adsorbed at the Au substrate.

More quantitatively, it is possible to simulate the surface reflection−absorption infrared spectra in Figure 3 as outlined in the Experimental Section. The results of these simulations are shown in Figure 3, summarized in Table 1 and represented diagramatically in Scheme 4. In particular, these simulations predict that the molecules constituting a crystalline monolayer of **I** are

Table 1. Characterization of Monolayers of Alkylthiols Adsorbed at a Crystalline Gold Substrate

	I $(HS-(CH_2)_{11}CH_3)$	**II** $(HS-(CH_2)_{10}COOH)$
Ellipsometry		
av film thickness, Å	20 ± 2	23 ± 2
calcd film thickness, Å	19.9	19.5
Surface Polarized Reflectance Infrared Spectrometry		
ν_{as} $(-CH_3)$, cm^{-1}	2964 ± 1	
ν_{as} $(-CH_2-)$, cm^{-1}	2918 ± 1 (0.0007 au)	2920 ± 1 (0.0006 au)
ν_s $(-CH_3)$, cm^{-1}	2878 ± 1	
ν_s $(-CH_2-)$, cm^{-1}	2851 ± 1	2849 ± 1
tilt (α), deg	+22 ± 1	+18 ± 1
twist (β), deg	−49 ± 2	+47 ± 2
azimuth (ψ),[a] deg	0	0

[a] Under the reported experimental conditions the measured spectrum is not sensitive to this (isotropic) parameter, and the indicated value was assumed.

tilted and twisted at angles of 22 ± 1° and −49 ± 2°, respectively. Similarly, those constituting a monolayer of **II** are tilted and twisted at angles of 18 ± 1° and 47 ± 2°, respectively. It is noted that the values reported here are in good agreement with those previously reported by Parikh and Allara for **I** and closely related molecules.[15]

Preparation and Characterization of Monolayer of TiO_2 Nanocrystallites Self-Assembled at a Modified Gold Substrate Using a Two-Step Method. The samples in Figure 3 were immersed in an ethanolic colloid of TiO_2 nanocrystallites for 4 h, washed thoroughly with ethanol, and dried in a stream of dry nitrogen. Initial characterization of these samples was by ellipsometry, surface reflection−absorption infrared spectroscopy and XPS spectroscopy.

The ellipsometric studies indicate that there is no change in the average thickness of the organic layer of **I** (20 ± 2 Å) deposited on Au following exposure to the ethanolic colloid; see Table 2. On the other hand, the average thickness of the organic layer of **II** increases by 4 Å (27 ± 2 Å); see Table 2. This apparent increase is likely due, as discussed below, to adsorption of TiO_2 nanocrystallites at this surface and limitations in the model used to fit the measured data.

The corresponding surface reflection−absorption infrared spectra, measured using p-polarized light, also indicate that there is no significant change in the average thickness or in the degree of crystallinity of the deposited monolayer; see Figure 4 and Table 2. In support of these findings, simulations of the measured spectra indicate only small changes in the measured twist or tilt angles; see also Figure 4. In short, there appears to be no significant change in the thickness or structure of the crystalline organic monolayers of **I** or **II** on Au following their immersion in an ethanolic colloid of TiO_2 nanocrystallites.

It is well established that a strong Lewis base, particularly one containing oxygen atoms, may be chemisorbed at the surface of colloidal TiO_2 nanocrystallites in ethanol.[26] Consequently, it was expected that immersion of a crystalline monolayer of **I** on Au in an ethanolic colloid of TiO_2 nanocrystallites would not be accompanied by adsorption of nanocrystallites. Equally,

(26) (a) Frei, H.; Fitzmaurice, D.; Grätzel, M. *Langmuir* **1990**, *6*, 198. (b) Moser, J.; Punchihewa, S.; Infelta, P.; Grätzel, M. *Langmuir* **1991**, *7*, 3012.

Scheme 4

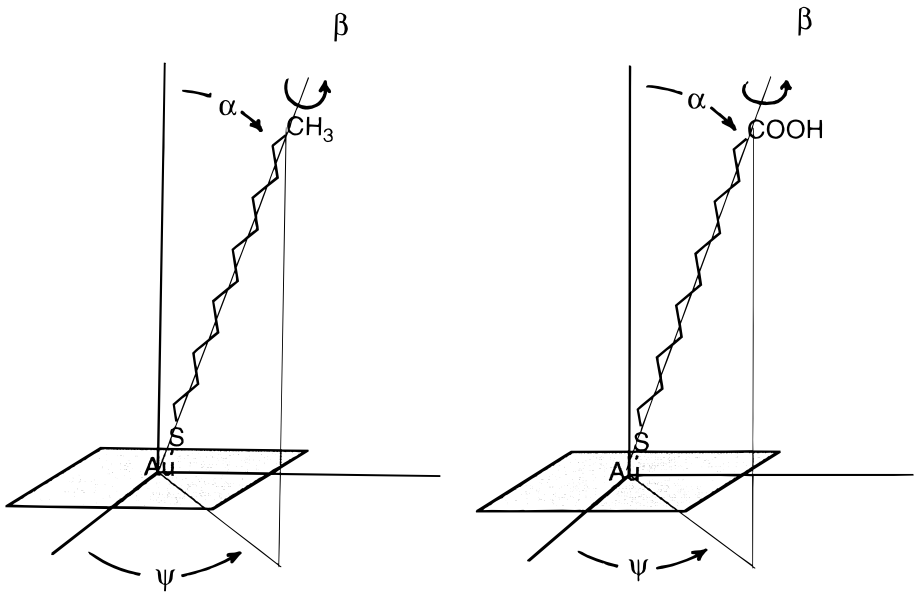

Table 2. Characterization of Monolayers of Alkylthiols Adsorbed at a Crystalline Gold Substrate and Treated with an Ethanolic TiO_2 Colloid

	I ($HS-(CH_2)_{11}CH_3$)	II ($HS-(CH_2)_{10}COOH$)
Ellipsometry		
av film thickness, Å	20 ± 2	27 ± 2
calcd film thickness, Å	19.9	19.4
Surface Polarized Reflectance Infrared Spectrometry		
ν_{as} ($-CH_3$), cm^{-1}	2964 ± 1	
ν_{as} ($-CH_2-$), cm^{-1}	2918 ± 1 (0.0006 au)	2920 ± 1 (0.0006 au)
ν_s ($-CH_3$), cm^{-1}	2878 ± 1	
ν_s ($-CH_2-$), cm^{-1}	2851 ± 1	2849 ± 1
tilt (α), deg	+20 ± 1	+18 ± 1
twist (β), deg	−49 ± 2	+47 ± 2
azimuth (ψ),[a] deg	0	0

[a] Under the reported experimental conditions the measured spectrum is not sensitive to this (isotropic) parameter, and the indicated value was assumed.

it was expected that after adsorption of TiO_2 nanocrystallites would be observed a crystalline monolayer of **II** on Au. To determine whether these expectations were justified, XPS was used to analyze for the presence of adsorbed TiO_2 nanocrystallites.

The survey XPS spectra of a crystalline monolayer of **I** on Au, measured both prior to and following its immersion in an ethanolic colloid of TiO_2 nanocrystallites, are not significantly different and contain the expected features.[27] The survey spectrum of crystalline monolayer of **I** on Au, following its immersion in an ethanolic colloid of TiO_2 nanocrystallites, is shown in Figure 5a. The following features are observed: peaks at 84, 88, 335, 353, and 547 eV assigned to the $4f_{7/2}$, $4f_{5/2}$, $4d_{5/2}$, $4d_{3/2}$, and $4p_{3/2}$ core levels of Au, respectively; peaks at 165 and 228 eV assigned to the 2p and 2s cores of S, respectively; a peak at 285 eV assigned to the 1s core of C. It is noted that a peak at 531 eV assigned to the 1s core of O is also observed. No peaks that would indicate the presence of adsorbed TiO_2 nanocrystallites are observed; see the higher resolution scan between 440 and 490 eV also in Figure 5a. On this basis it is concluded that no TiO_2 nanocrystallites are adsorbed at this substrate.

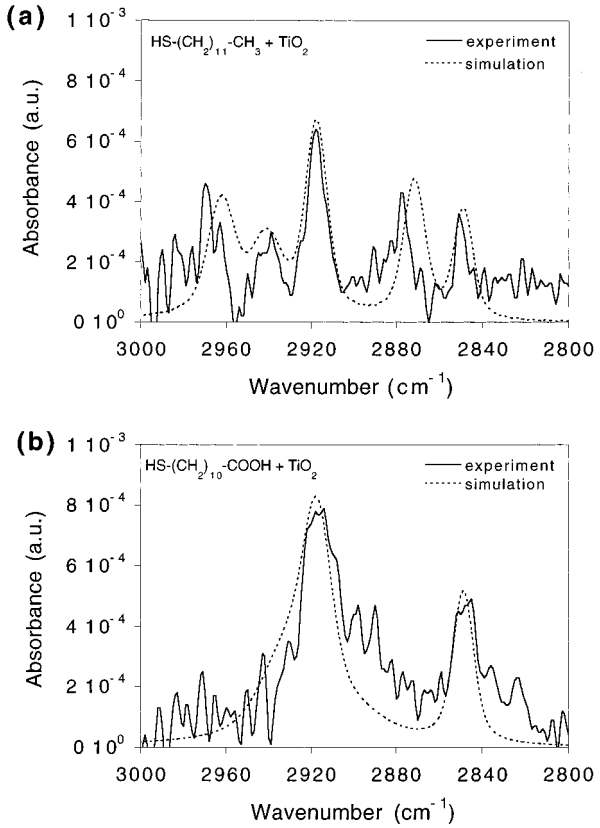

Figure 4. (a) Surface reflection−absorption infrared spectrum, measured using p-polarized light at an incident angle of 85°, of a crystalline monolayer of $HS-(CH_2)_{11}-CH_3$ adsorbed at an annealed gold substrate similar to that in Figure 2 following immersion for 4 h in an ethanolic TiO_2 colloid similar to that in Figure 1. Also shown is the simulated spectrum. (b) As in (a) for a crystalline monolayer of $HS-(CH_2)_{10}-COOH$ adsorbed at an annealed Au substrate similar to that in Figure 2.

(27) Moulder, J.; Stickle, W.; Sobol, P.; Bomben, K. *Handbook of X-ray Photoelectron Spectroscopy*; Chastain, J., Ed.; Perkin-Elmer Corp.: Eden Prairie, 1992.

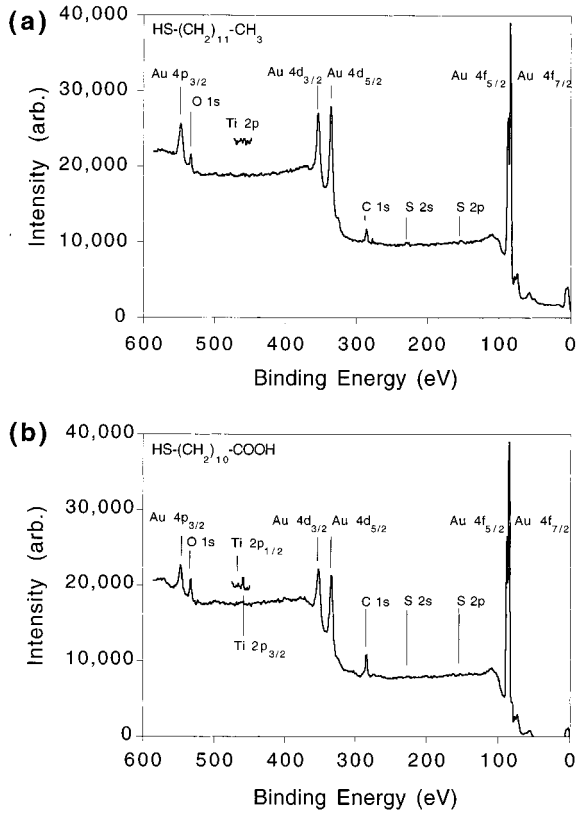

Figure 5. (a) Survey X-ray photoelectron spectrum, measured using the Kα X-ray emission of aluminum at 1486.6 eV and detected at a takeoff angle of 15°, of a crystalline monolayer of $HS-(CH_2)_{11}-CH_3$ adsorbed at an annealed gold substrate similar to that in Figure 2 following immersion for 4 h in an ethanolic TiO_2 colloid similar to that in Figure 1. Also shown is a higher resolution scan for the same sample between 440 and 490 eV. (b) As in (a) for a crystalline monolayer of $HS-(CH_2)_{10}-COOH$ adsorbed at an annealed Au substrate similar to that in Figure 2 following immersion for 4 h in an ethanolic TiO_2 colloid similar to that in Figure 1.

A survey XPS spectrum was also measured for a crystalline monolayer of **II** on Au prior to immersion in an ethanolic colloid containing TiO_2 nanocrystallites and agrees well with that measured for a monolayer of **I** on Au under the same conditions.[27] The spectrum measured for a crystalline monolayer of **II** on Au following immersion in an ethanolic colloid containing TiO_2 nanocrystallites is shown in Figure 5b and agrees well with that measured for a monolayer of **I** on Au under the same conditions with the following exception: Additional peaks at 458 and 464 eV assigned to the $2p_{3/2}$ and $2p_{1/2}$ core levels of Ti are observed; see also the higher resolution scan between 440 and 490 eV in Figure 5b, on which basis it is concluded that TiO_2 nanocrystallites are adsorbed at this substrate.

The above studies have been complemented by high-resolution XPS studies, also at a takeoff angle of 15°. These results of these studies for a monolayer of **II** on Au following immersion in an ethanolic colloid of TiO_2 nanocrystallites are summarized in Table 3 and Figure 6 and discussed below.

The peaks assigned to the $4f_{7/2}$ and $4f_{5/2}$ core levels of the Au atoms of the substrate are shown in Figure 6a. These are observed at 84.0 and 87.7 eV, respectively, in excellent agreement with values reported in the literature.[27] On the basis of these results it is possible to conclude that charging of this substrate is not significant.[7a]

Table 3. Characterization by High-Resolution XPS of Monolayers of an Alkylthiol ($HS-(CH_2)_{10}COOH$) Adsorbed at a Crystalline Gold Substrate and Treated with an Ethanolic Colloid of TiO_2 Nanocrystallites

atom core level	binding energy[a] (eV)
Au 4f 7/2	84.0 Au bulk
5/2	87.7 Au bulk
S 2p unresolved	162.5 $-S-$Au
	169.4 $-SO_3H$ etc.
C 1s	285.0 $-CH_2-$
	285.8 $-CH_2-$COOH
	287.2 $-CH_2-$S−Au
	289.3 −COOH
Ti 2p 3/2	459.4 TiO_2 bulk
1/2	465.6 TiO_2 bulk

[a] The spectra from which the reported binding energies were determined are plotted in Figure 6 and were recorded at a takeoff angle of 15°.

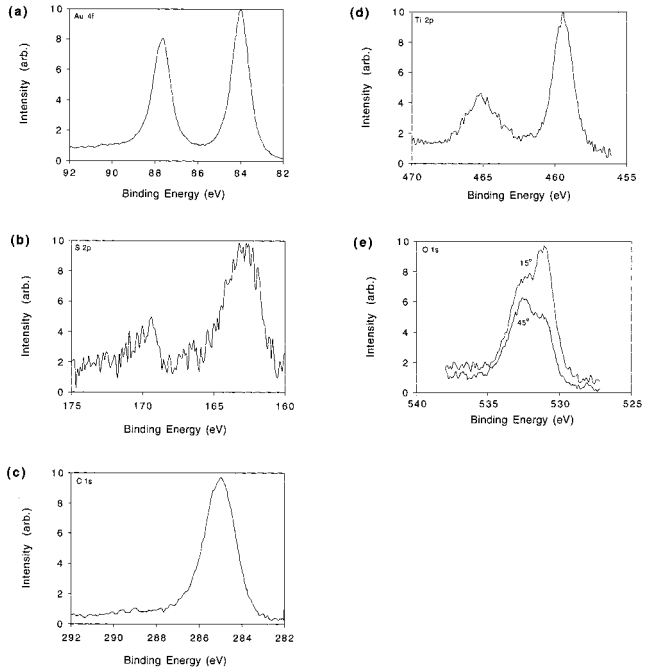

Figure 6. High-resolution X-ray photoelectron spectra, measured using the Kα X-ray emission of aluminum at 1486.6 eV and detected at a takeoff angle of 15°, of a crystalline monolayer of $HS-(CH_2)_{10}-COOH$ adsorbed at an annealed gold substrate similar to that in Figure 2 following immersion for 4 h in an ethanolic TiO_2 colloid similar to that in Figure 1. Peaks assigned to the following atoms are shown: (a) Au 4f; (b) S 2p; (c) C 1s; (d) Ti 2p; (e) O 1s (15° and 45°).

The peaks assigned to the unresolved $2p_{3/2,1/2}$ core levels of the S atom of **II** adsorbed at the Au substrate are shown in Figure 6b. The peak at 162.8 eV is assigned to the 2p core of a metal sulfide, i.e., to the S atom bonded directly to the Au atom. The peak at 169.4 eV is assigned to the 2p core of a sulfate or sulfonic acid moiety.[27,28] The presence of this latter peak, it has been suggested, indicates that a fraction of the thiol present has been oxidized as a result of exposure to air or the spectrometer source.[7a,28] The presence in the survey spectrum of the crystalline monolayer of **I** on Au of a peak that may be assigned to the 1s core of the O atom is also consistent with this suggestion; see Figure 5a.

(28) (a) Nuzzo, R.; Zegarski, B.; Dubois, L. *J. Am. Chem. Soc.* **1987**, *109*, 733. (b) Laibinis, P.; Whitesides, G.; Allara. D.; Tao, Y.-T.; Parikh, A.; Nuzzo, R. *J. Am. Chem. Soc.* **1991**, *113*, 7152.

The peak assigned to the 1s core of the C atoms of **II** are shown in Figure 6c. This broad feature may be decomposed into four discrete peaks assigned to the 1s cores of the following C atoms: First, a peak at 285.0 eV assigned to the C atoms in the $-CH_2-$ groups of the alkyl chain of **II**; second, a peak at 285.8 eV assigned to the C atom in the $-CH_2-$ group α to the terminal −COOH group; third, a peak at 289.3 eV assigned to the C atom of the terminal −COOH group, denoted −C(COOH); and finally, a peak at 287.2 eV assigned to the C atom in the $-CH_2-$ group α to the terminal −S− Au link, denoted C(S).[8a,27]

The peaks assigned to the $2p_{3/2}$ and $2p_{1/2}$ core levels of the Ti atoms of the adsorbed TiO_2 nanocrystallites are shown in Figure 6d. The peak at 459.4 eV is assigned to the $2p_{3/2}$ level of a Ti atom in TiO_2. The peak at 465.6 eV is assigned to the $2p_{1/2}$ level of a Ti atom in TiO_2. Both these values are in excellent agreement with those expected for bulk TiO_2.[8,27]

Finally, we consider the peaks assigned to the 1s core of the O atom and shown in Figure 6e. As stated above, some fraction of the thiol present may have been oxidized, either by exposure to air or as a result of exposure to the XPS source, and a component of this signal is likely due to the presence of sulfate or sulfonic acid moieties. In addition, there will be a component of this signal that is due to the oxygen atoms present in the −COOH group of **II**. Finally, there will be a contribution due to the O atoms present in the TiO_2 nanocrystallites. As a consequence a definitive assignment of the observed peaks is not possible with the data available. However, of the two peaks that are resolved at 531.0 and 532.7 eV, the former is tentatively assigned to O atoms in the TiO_2 nanocrystallites,[8b,c,27] while the latter likely contains contributions from the O atoms of the −COOH group and oxidized thiols.[8,27,30] Further support for the above assignments comes from the observation that, as expected, the peak assigned to the 1s core of O atoms of TiO_2 (531.0 eV) shows greater sensitivity to the takeoff angle than the peak assigned to the 1s core of the O atoms of the −COOH group and oxidized thiols (532.7 eV); see Figure 6e.

It is clear from the above studies that TiO_2 nanocrystallites are adsorbed at a monolayer of **II**, itself adsorbed at a Au substrate. Further, since it has been established that the structure of the crystalline monolayer of **II** on Au is unaltered following exposure to an ethanolic TiO_2 colloid, it is reasonable to assume that these nanocrystallites are adsorbed at the surface of the adsorbed monolayer of **II**.

Direct confirmation of the above has proved possible by high-resolution angle-dependent XPS studies at takeoff angles of 45°, 15°, 5°, 3°, and 1°. The findings of these studies are discussed below and summarized in Table 4 and Figure 7.

Plotted in Figure 7a is the angle dependence of the ratios of the percentage atomic concentrations of Au, S, C, Ti, and O in relevant combinations for a monolayer of **II** on a crystalline Au substrate following immersion in an ethanolic colloid of TiO_2 nanocrystallites. In general, as the takeoff angle, or the angle between the surface and the electrons accepted by the analyzer, is decreased, the surface sensitivity of XPS increases. On this basis,[31] it would be predicted that if the monolayer is formed by adsorption of the thiol moiety at the Au substrate and adsorption of TiO_2 nanocrystallites at the carboxylate moiety that the ratio of Ti/Au and Ti/S would increase as the takeoff angle deceased. However, it would also be predicted that while the ratio of Ti/O would be largely independent of the takeoff angle, the ratio of S/Au would increase at lower takeoff angles. Finally, it would also be predicted that while the ratio of C/O would be largely independent of the takeoff angle, the ratio of C/S would increase at lower takeoff angles. All of these predictions are confirmed by the data plotted in Figure 7a.

Table 4. Characterization by High-Resolution Angle-Dependent XPS of a Monolayer of an Alkylthiol ($HS-(CH_2)_{10}COOH$) Adsorbed at a Crystalline Gold Substrate and Treated with an Ethanolic Colloid of TiO_2 Nanocrystallites

takeoff angle (deg)	atomic concentration (%)				
	Au4f	S2p	C1s	O1s	Ti2p
45	21.92	4.07	51.22	18.18	4.60
15	13.21	3.17	55.48	21.83	6.31
5	8.87	2.86	56.58	23.67	8.03
3	7.44	2.91	58.97	22.65	8.04
1	6.48	2.83	56.28	26.30	8.12

ratio of atomic concentrations[a]	takeoff angle (deg)				
	45	15	5	3	1
Ti/Au	0.21	0.48	0.90	1.07	1.25
Ti/S	1.13	1.99	2.81	2.76	2.87
Ti/O	0.25	0.29	0.34	0.36	0.31
S/Au (×2.0)	0.36	0.48	0.64	0.78	0.88[b]
C/O	2.81	2.54	2.39	2.60	2.14
C/S (×0.2)	2.52	3.50	3.95	4.05	3.98[b]
C(COOH)/Ti	0.90	0.39	0.38	0.34	0.42
C(COOH)/Au	0.19	0.19	0.36	0.32	0.57
C(S)/Ti	1.01	0.58	0.43	0.72	0.52
C(S)/Au	0.21	0.28	0.41	0.68	0.70

[a] The error in the reported values is less than 5%. [b] These data were scaled as indicated to aid clarity of presentation in Figure 7.

In a more detailed analysis of these data, the angle dependence of the ratios of the percentage atomic concentrations of C(S), C(COOH), Au, and Ti were plotted in relevant combinations for the sample in Figure 7a; see Figure 7b. It would be predicted that if the monolayer is formed by adsorption of the thiol moiety at the Au substrate and adsorption of TiO_2 nanocrystallites at the carboxylic acid moiety that the ratio of C(S)/Au and C(S)/Ti would increase and decrease respectively as the takeoff angle deceased. However, it would also be predicted that the ratio of C(COOH)/Au and C(COOH)/Ti would increase and decrease, respectively. All of these predictions are confirmed by the data plotted in Figure 7b.

The final question to be addressed in this section is the extent of coverage of the sample by the adsorbed TiO_2 nanocrystallites. To this end, samples similar to those described above were prepared and studied, both prior to and following immersion in an ethanolic colloid of TiO_2 nanocrystallites, by RBS. It should be noted

(29) Evans, S.; Ulman, A.; Goppert-Berarducci, K.; Gerenser, L. *J. Am. Chem. Soc.* **1991**, *113*, 5866.

(30) Herdt, G.; Jung, D.; Czanderna, A. *Prog. Surf. Sci.* **1995**, *50*, 103.

(31) (a) Bain, C.; Troughton, E.; Tao, Y.-T.; Evall, J.; Whitesides, G.; Nuzzo, R. *J. Am. Chem. Soc.* **1989**, *111*, 321. (b) Briggs, D.; Riviere, J. In *Practical Surface Analysis*; Briggs, D., Seah, M., Ed.; Wiley: Chichester, 1990; Vol. I, pp 134−136.

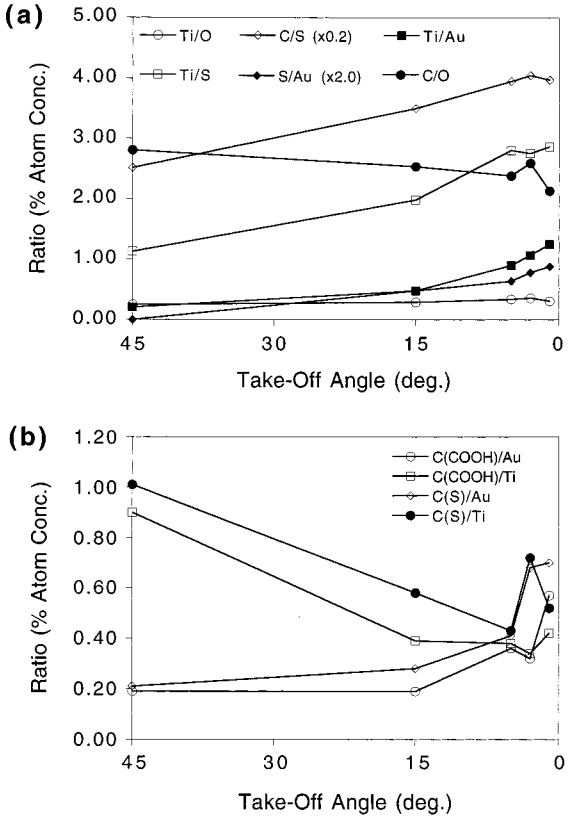

Figure 7. (a) Dependence of the ratios of the percentage atomic concentration of the indicated elements on takeoff angle as determined from a high-resolution X-ray photoelectron spectrum, measured using the Kα X-ray emission of aluminum at 1486.6 eV, of a crystalline monolayer of $HS-(CH_2)_{10}-COOH$ adsorbed at an annealed gold substrate similar to that in Figure 2 following immersion for 4 h in an ethanolic TiO_2 colloid similar to that in Figure 1. (b) As in (a) for the C(S) and C(COOH), Ti and Au atoms of a crystalline monolayer of $HS-(CH_2)_{10}-COOH$ adsorbed at an annealed gold substrate similar to that in Figure 2 following immersion for 4 h in an ethanolic TiO_2 colloid similar to that in Figure 1.

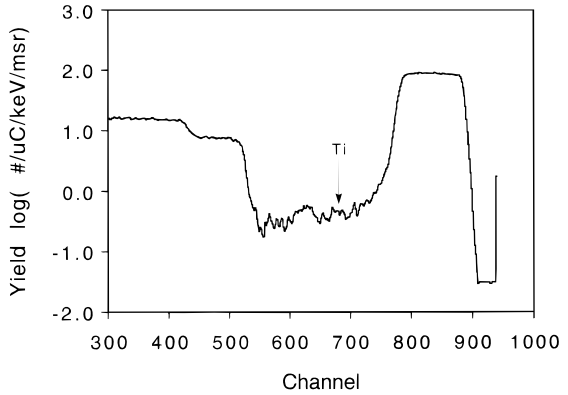

Figure 8. Rutherford backscattering spectrum, recorded using He^+ (2 MeV) for a sample whose surface is at 50° to the incident beam, of a crystalline monolayer of $HS-(CH_2)_{10}-COOH$ adsorbed at an annealed Au substrate following immersion for 4 h in an ethanolic TiO_2 colloid similar to that in Figure 1.

that the samples studied were washed thoroughly with ethanol and dried in a stream of dry nitrogen following immersion in the ethanolic colloid.

Shown in Figure 8 is the RBS of an annealed Au substrate modified by a monolayer of **II** following immersion in an ethanolic colloid of TiO_2 nanocrystallites for 4 h. From this spectrum the surface coverage

Scheme 5

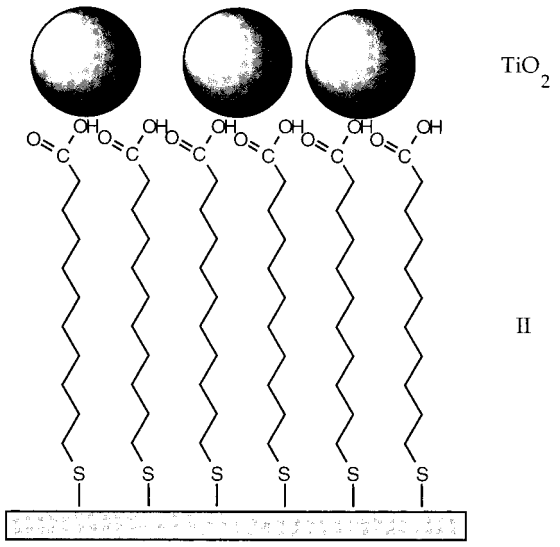

Two-Step Method

of Ti atoms was calculated to be 2×10^{15} cm^{-2}. This finding is consistent with a coverage of 0.7 of a monolayer of 22 Å diameter TiO_2 nanocrystallites.

In short it is possible to conclude that the structure of the assembled monolayer is as represented in Scheme 5.

Preparation and Characterization of Monolayer of Modified TiO_2 Nanocrystallites Self-Assembled at a Gold Substrate Using a One-Step Method. A closely related approach to the preparation of monolayers of nanocrystallites on a crystalline Au substrate is the following:[7] An ethanolic colloid of TiO_2 nanocrystallites is prepared in the presence of **II**, the latter being adsorbed at the surface of the nanocrystallite via the carboxylic acid moiety.[26] These nanocrystallites are then adsorbed at the crystalline Au substrate via the thiol moiety of **II**. In practice a Au substrate is immersed in an ethanolic colloid of TiO_2 nanocrystallites prepared in the presence of **II** for 4 h, washed thoroughly with ethanol, and dried in a stream of dry nitrogen. Initially these samples were characterized by surface reflection−absorption infrared spectroscopy and by XPS spectroscopy. It should be noted that characterization of these samples by ellipsometry on the basis of a multilayer model did not yield reliable results.

Shown in Figure 9a is the surface reflection−absorption infrared spectrum, measured using p-polarized light, of the modified substrate prepared as described above. It is noted, that the frequency of the asymmetric (2926 cm^{-1}, 0.0010 au) and symmetric (2858 cm^{-1}, 0.0005 au) stretches are characteristic of the liquid state, while the corresponding absorbances are approximately twice those expected for a monolayer.[24] In short, it is clear that the molecules of **II** adsorbed at the crystalline Au substrate are not present as an organized monolayer.

Shown in Figure 9b is the corresponding survey XPS spectrum. It is noted, that peaks confirming the presence of Au, S, C, Ti, and O are observed.[27] Further, from a higher resolution scan between 440 and 490 eV shown in Figure 9b, peaks at 458 and 464 eV are assigned to the $2p_{3/2}$ and $2p_{1/2}$ core levels of Ti, respectively.[8,27] On

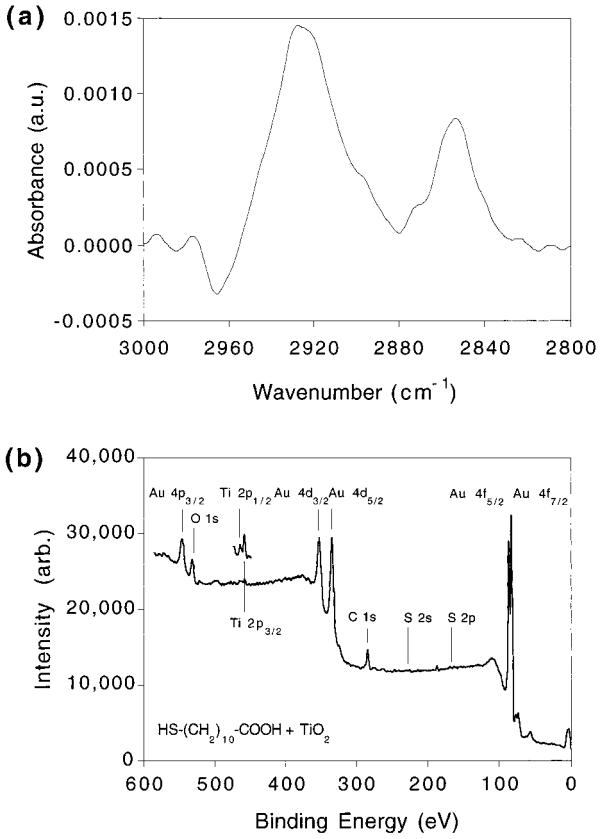

Figure 9. (a) Surface reflection−absorption infrared spectrum, measured using p-polarized light at an incident angle of 85°, of TiO_2 nanocrystallites modified by chelated HS−$(CH_2)_{10}$−COOH and adsorbed at an annealed gold substrate similar to that in Figure 2 from an ethanolic colloid during 4 h. (b) Survey X-ray photoelectron spectrum, measured using the Kα X-ray emission of aluminum at 1486.6 eV and detected at a takeoff angle of 15°, of sample in (a). Also shown is a higher resolution scan for the same sample between 440 and 490 eV.

Table 5. Characterization by High-Resolution XPS of a Crystalline Gold Substrate Treated with an Ethanolic Colloid of TiO_2 Nanocrystallites Modified by an Adsorbed Alkylthiol (HS−$(CH_2)_{10}$COOH)

atom core level	binding energy[a] (eV)
Au 4f 7/2	84.0 Au bulk
5/2	87.7 Au bulk
S 2p unresolved	162.6 −*S*−Au
	169.1 −SO_3H etc.
C 1s	285.0 −CH_2−
	285.7 −CH_2−COOH
	287.0 −CH_2−S−Au
	289.2 −COOH
Ti 2p 3/2	459.3 *Ti*O_2 bulk
1/2	465.4 *Ti*O_2 bulk

[a] The spectra from which the reported binding energies were determined are plotted in Figure 10 and were recorded at a takeoff angle of 15°.

the basis of the above findings, it is concluded that the modified TiO_2 nanocrystallites are adsorbed at the crystalline Au substrate but in a manner that does not result in formation of an organized monolayer of **II**.

To further characterize the Au substrate at which the modified nanocrystallites had been adsorbed, high-resolution XPS studies were undertaken at a takeoff angle of 15°. The findings of these studies, summarized in Table 5 and Figure 10, agree well with the findings of similar studies reported above for the sample prepared using the two-step method.

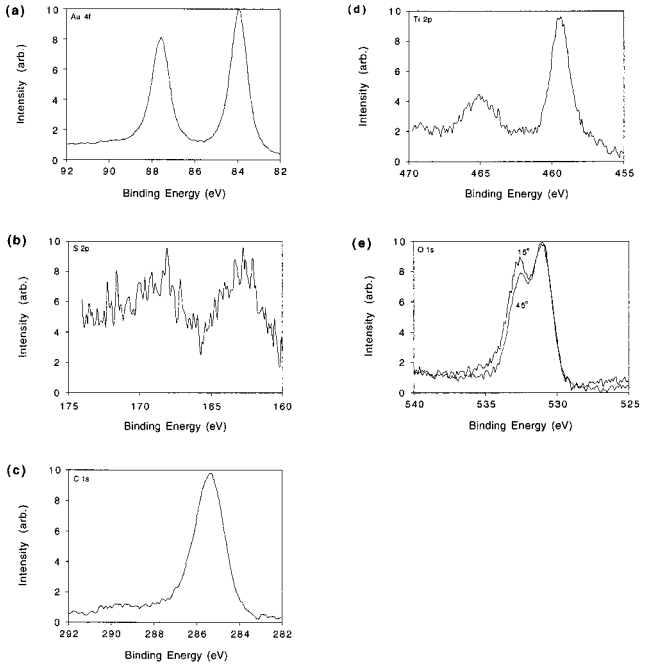

Figure 10. High-resolution X-ray photoelectron spectra, measured using the Kα X-ray emission of aluminum at 1486.6 eV and detected at a takeoff angle of 15°, of TiO_2 nanocrystallites modified by chelated HS−$(CH_2)_{10}$−COOH and adsorbed at an annealed gold substrate similar to that in Figure 2 from an ethanolic colloid during 4 h. Peaks assigned to the following atoms are shown: (a) Au 4f; (b) S 2p; (c) C 1s; (d) Ti 2p; (e) O 1s (15° and 45°).

Table 6. Characterization by High-Resolution Angle-Dependent XPS of a Crystalline Gold Substrate Treated with an Ethanolic Colloid of TiO_2 Nanocrystallites Modified by an Adsorbed Alkylthiol (HS−$(CH_2)_{10}$COOH)

takeoff angle (deg)	atomic concentration (%)				
	Au4f	S2p	C1s	O1s	Ti2p
45	16.64	4.89	49.41	20.15	6.54
15	7.02	2.56	59.96	22.50	6.24
5	3.29	3.28	67.77	20.63	5.02
3	3.32	3.24	67.66	22.21	4.57
1	2.91	4.07	66.65	20.83	5.44

ratio of atomic concentrations[a]	takeoff angle (deg)				
	45	15	5	3	1
Ti/Au	0.39	0.89	1.53	1.38	1.87
Ti/S	1.33	3.77	1.53	1.41	1.14
Ti/O	0.32	0.28	0.28	0.21	0.26
S/Au (×2.0)	0.59	0.73	1.99	1.95	2.80[b]
C/O	2.45	2.66	3.28	3.05	3.20
C/S (×0.2)	2.02	4.68	4.13	4.17	3.27[b]
C(COOH)/Ti	0.47	0.38	0.35	0.54	0.45
C(COOH)/Au	0.18	0.52	1.35	2.63	2.67
C(S)/Ti	0.43	0.58	0.43	0.72	0.52
C(S)/Au	0.04	0.22	0.61	0.65	1.40

[a] The error in the reported values is less than 5%. [b] These data were scaled as indicated to aid clarity of presentation in Figure 11.

Additional, high-resolution angle-dependent XPS studies were undertaken at takeoff angles of 45°, 15°, 5°, 3°, and 1°. The findings of these studies, summarized in Table 6 and Figure 11, are discussed in detail below.

Plotted in Figure 11a are the ratios of the percentage atomic concentrations of Au, S, C, Ti, and O in relevant combinations for a range of takeoff angles. As stated, decreasing the takeoff angle increases the surface sensitivity of XPS. On this basis,[31] it would be predicted

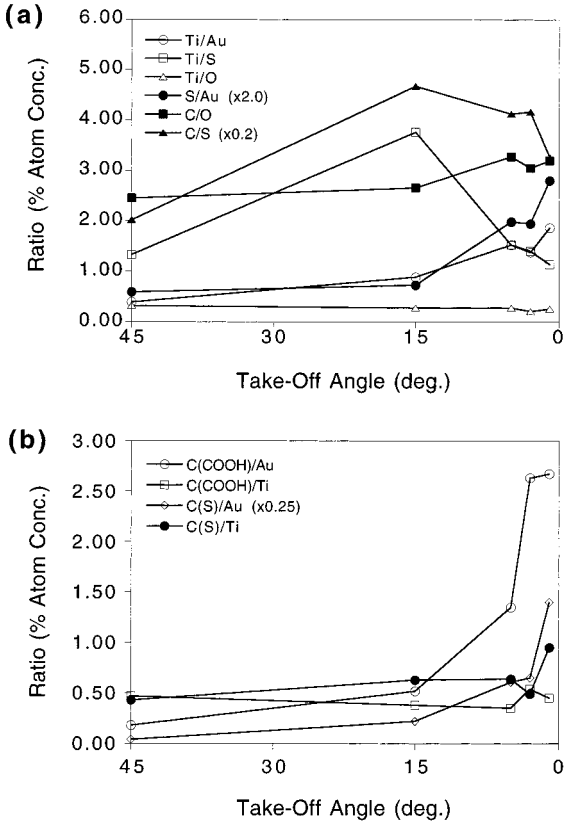

Figure 11. (a) Dependence of the ratios of the percentage atomic concentration of the indicated elements on takeoff angle for a high-resolution X-ray photoelectron spectrum, measured using the Kα X-ray emission of aluminum at 1486.6 eV, of TiO_2 nanocrystallites modified by chelated $HS-(CH_2)_{10}-COOH$ and adsorbed at an annealed gold substrate similar to that in Figure 2 from an ethanolic colloid during 4 h. (b) As in (a) for the C(S) and C(COOH), Ti and Au atoms of a crystalline monolayer of TiO_2 nanocrystallites modified by chelated $HS-(CH_2)_{10}-COOH$ and adsorbed at an annealed gold substrate similar to that in Figure 2 from an ethanolic colloid during 4 h.

that for modified TiO_2 nanocrystallites adsorbed at a crystalline Au substrate the ratio of Ti/Au would increase as the takeoff angle deceased. This is observed to be the case. In the case of TiO_2 nanocrystallites adsorbed at a crystalline monolayer of **II**, it was predicted that the Ti/S ratio would also increase as the takeoff angle decreased and was observed to be the case. However, here it would be predicted that since the functionalized thiols linked to the surface of the nanocrystallite may be oriented both into and away from the Au substrate that a more complex relationship would be observed. Consistent with this expectation, it is observed that initially the Ti/S ratio increases and then decreases, i.e., photoelectrons from the S atoms at the Au surface are detected initially while those from the S atoms oriented into the bulk solution are detected subsequently. On this basis, it would also be predicted that while the ratio of Ti/O would be largely independent of the takeoff angle, the ratio of S/Au would increase at lower takeoff angles. Finally, it would also be predicted that while the ratio of C/O would be largely independent of the takeoff angle, the ratio of C/S would initially increase and subsequently decrease at lower takeoff angles. All of these predictions are confirmed by the data plotted in Figure 11a.

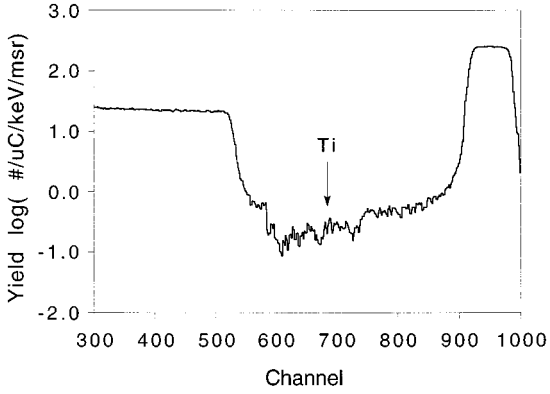

Figure 12. Rutherford backscattering spectrum, recorded using He^+ (2 MeV) for a sample whose surface is at 50° to the incident beam, of an annealed Au substrate following immersion for 4 h in an ethanolic colloid of TiO_2 nanocrystallites modified by adsorbed $HS-(CH_2)_{10}-COOH$.

In a more detailed consideration of these data, the angle dependence of the ratios of the percentage atomic concentrations of C(S), C(COOH), Au, and Ti were plotted in relevant combinations for the sample in Figure 11a; see Figure 11b. It would be predicted for modified TiO_2 nanocrystallites adsorbed at a crystalline Au substrate that the ratio of C(S)/Au and C(S)/Ti would increase and remain constant respectively as the takeoff angle decreased. It would also be predicted that the ratio of C(COOH)/Au and C(COOH)/Ti would increase and remain constant as the takeoff angle decreased. All these predictions are confirmed by the data plotted in Figure 11b.

The final question to be addressed in this section is the extent of coverage of the sample by the adsorbed TiO_2 nanocrystallites. To this end, samples similar to those described above were prepared and studied, both prior to an following immersion in an ethanolic colloid of TiO_2 nanocrystallites, by RBS. It should be noted that the samples studied were washed thoroughly with ethanol and dried in a stream of dry nitrogen following immersion in the ethanolic colloid.

Shown in Figure 12 is the RBS of an annealed Au substrate modified by immersion in an ethanolic colloid of TiO_2 nanocrystallites modified by adsorbed **II** for 4 h. From this spectrum the surface coverage of Ti atoms was calculated to be 1×10^{15} cm^{-2}. This finding is consistent with a coverage of 0.4 of a monolayer of 20 Å diameter TiO_2 nanocrystallites. It is noted, that due to the fact that the nanocrystallites adsorbed at the Au substrate are modified by adsorbed **II**, their distance of closest approach is limited and that the coverage will be less than that observed for a similar sample prepared using a two-step method.

In short it is possible to conclude that the structure of the assembled monolayer is as represented in Scheme 6.

Conclusions

Two approaches have been described that may be used to adsorb a monolayer of TiO_2 nanocrystallites from solution onto an annealed Au substrate. In the first of these, a two-step method, a crystalline monolayer of a functionalized thiol is first adsorbed at the annealed Au substrate. The modified substrate is then immersed in an ethanolic colloid of TiO_2 nanocrystallites. As the

Scheme 6

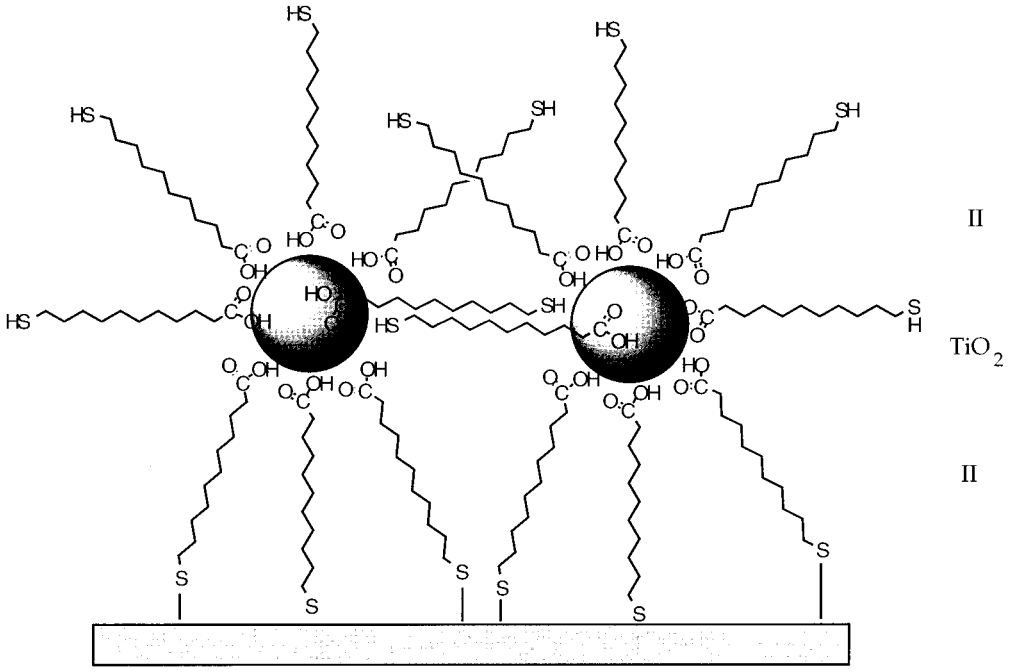

Scheme 7

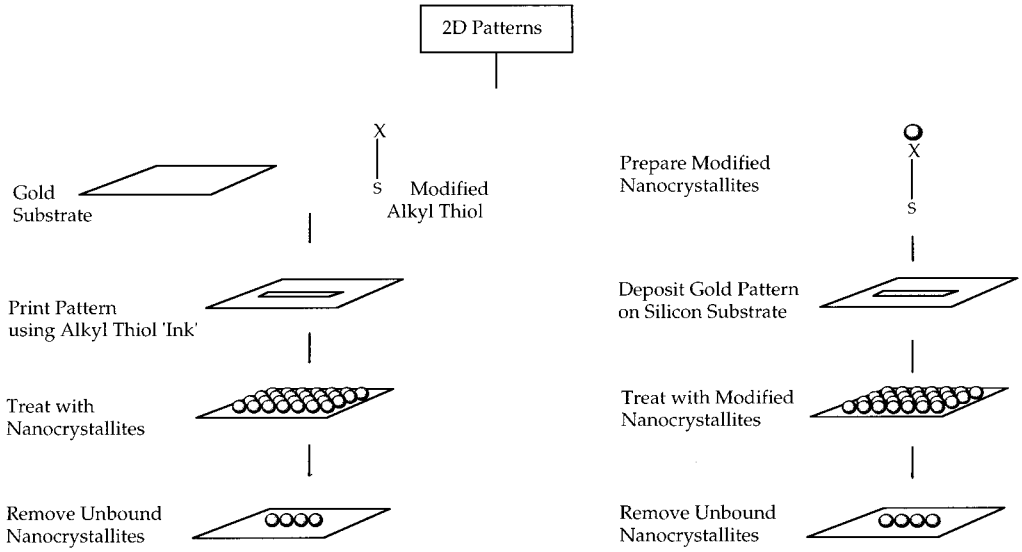

functionalized thiol has been modified with a terminal carboxylic acid group, known to be strongly adsorbed at TiO_2, the TiO_2 nanocrystallites are adsorbed at the modified Au substrate, see Schemes 2 and 5. In the second of these approaches, a one-step method, an annealed Au substrate is immersed in an ethanolic colloid of TiO_2 nanocrystallites modified by adsorption of a functionalized thiol. These nanocrystallites are subsequently adsorbed at the crystalline Au substrate; see Schemes 2 and 6. In each case the resulting monolayer possesses regions in which the adsorbed nanocrystallites are ordered although, long-range order is absent.

Current work is being directed toward the adsorption of TiO_2 nanocrystallites at patterned crystalline Au substrates using both the one-step and two-step methods reported here, see Scheme 7.[32] Adopting this approach it is hoped it will prove possible to self-assemble, from solution, complex patterns of TiO_2 nanocrystallites at a crystalline Au substrate.

These, and related studies,[33] are expected to facilitate the preparation of nanostructured semiconductor electrodes that are sufficiently well defined to the detailed

(32) Rizza, R.; Fitzmaurice, D., manuscript in preparation.
(33) Private communications.

study of charge carrier accumulation and transport in nanoporous−nanocrystalline materials. These studies also represent, together with related studies in a number of laboratories,[34] initial steps directed toward the self-assembly of solid-state devices in solution.

Acknowledgment. The authors wish to thank the staff of the National Microelectronics Research Centre, and in particular Dr. Patrick Kelly, for their assistance in undertaking the reported ellipsometric studies. The authors also wish to thank the staffs of the Electron Microscopy Centre at UCD and the National Metrology Laboratory at Forbairt for their assistance in undertaking the reported TEM and STM studies, respectively. The authors must also thank Drs. Allara, Heitpas, and Parikh for their assistance in simulating the reported surface reflection−absorption infrared spectra. The studies performed at UCD were supported by a grant from the Commission of the European Union under the Joule III program (Contract JOR3-CT96-0107). S.H. was funded as part of the Irish American Partnership Scholarship Program.

CM970349U

(34) (a) Murray, C.; Kagan, C.; Bawendi, M. *Science* **1995**, *270*, 1335. (b) Mirkin, B.; Letsinger, R.; Mucic, R.; Storhoff, J. *Nature* **1996**, *382*, 607. (c) Alivisatos, P.; Peng, X.; Wilson, T.; Johnson, K.; Loweth, C.; Bruchez, M.; Schultz, P. *Nature* **1996**, *382*, 609. (d) Cusack, L. Rizza, R.; Gorelov, A.; Fitzmaurice, D. *Angew. Chem., Int. Ed. Engl.* **1997**, *36*, 848.